

# Determination of fructose metabolic pathways in normal and fructose-intolerant children: A $^{13}\text{C}$ NMR study using $[\text{U-}^{13}\text{C}]$ fructose

(glucose  $^{13}\text{C}$ - $^{13}\text{C}$  coupling/phosphofructokinase/direct conversion of fructose 1-phosphate to fructose 1,6-bisphosphate)

ASHER GOPHER<sup>†</sup>, NACHUM VAISMAN<sup>‡</sup>, HANNA MANDEL<sup>§</sup>, AND AVIVA LAPIDOT<sup>†¶</sup>

<sup>†</sup>Department of Isotope Research, Weizmann Institute of Science, Rehovot, Israel; <sup>‡</sup>Department of Pediatrics, Kaplan Hospital, Rehovot, Israel; and

<sup>§</sup>Department of Pediatrics, Rambam Hospital, Haifa, Israel

Communicated by Mildred Cohn, April 12, 1990

**ABSTRACT** An inborn deficiency in the ability of aldolase B to split fructose 1-phosphate is found in humans with hereditary fructose intolerance (HFI). A stable isotope procedure to elucidate the mechanism of conversion of fructose to glucose in normal children and in HFI children has been developed. A constant infusion of D- $[\text{U-}^{13}\text{C}]$ fructose was given nasogastrically to control and to HFI children. Hepatic fructose conversion to glucose was estimated by examination of  $^{13}\text{C}$  NMR spectra of plasma glucose. The conversion parameters in the control and HFI children were estimated on the basis of doublet/singlet values of the plasma  $\beta$ -glucose C-1 splitting pattern as a function of the rate of fructose infusion (0.26–0.5 mg/kg per min). Significantly lower values ( $\approx 3$ -fold) for fructose conversion to glucose were obtained for the HFI patients as compared to the controls. A quantitative determination of the metabolic pathways of fructose conversion to glucose was derived from  $^{13}\text{C}$  NMR measurement of plasma  $[\text{U-}^{13}\text{C}]$ glucose isotopomer populations. The finding of isotopomer populations of three adjacent  $^{13}\text{C}$  atoms at glucose C-4 ( $^{13}\text{C}_3$ - $^{13}\text{C}_4$ - $^{13}\text{C}_5$ ) suggests that there is a direct pathway from fructose, by-passing fructose-1-phosphate aldolase, to fructose 1,6-bisphosphate. The metabolism of fructose by fructose-1-phosphate aldolase activity accounts for only  $\approx 50\%$  of the total amount of hepatic fructose conversion to glucose. It is suggested that phosphorylation of fructose 1-phosphate to fructose 1,6-bisphosphate by 1-phosphofructokinase occurs in human liver (and intestine) when fructose is administered nasogastrically; 47% and 27% of the total fructose conversion to glucose in controls and in HFI children, respectively, takes place by way of this pathway. In view of the marked decline by 67% in synthesis of glucose from fructose in HFI subjects found in this study, the extent of  $[\text{U-}^{13}\text{C}]$ glucose formation from a "trace" amount ( $\approx 20$  mg/kg) of  $[\text{U-}^{13}\text{C}]$ fructose infused into the patient can be used as a safe and noninvasive diagnostic test for inherent faulty fructose metabolism.

Early studies on fructose metabolism in liver and muscle led to the conclusion that these tissues have an enzyme system capable of converting fructose 1-phosphate (Fru-1-P) to fructose 1,6-bisphosphate  $[\text{Fru}(1,6)\text{P}_2]$  (1). Hers (2) found that, in rat liver, this conversion involves cleavage of Fru-1-P to dihydroxyacetone phosphate and D-glyceraldehyde, with subsequent phosphorylation and condensation to form  $\text{Fru}(1,6)\text{P}_2$ . The lack of isotope equilibrium between glucose C-1 and C-6 was attributed to incomplete equilibration between dihydroxyacetone phosphate and glyceraldehyde 3-phosphate at the triose-phosphate isomerase reaction; hence the existence of a direct pathway, such as phosphorylation of Fru-1-P to  $\text{Fru}(1,6)\text{P}_2$ , to account for this disequilibrium was not considered (3).

The publication costs of this article were defrayed in part by page charge payment. This article must therefore be hereby marked "advertisement" in accordance with 18 U.S.C. §1734 solely to indicate this fact.

An inborn deficiency in the ability of aldolase B to split Fru-1-P is found in humans with hereditary fructose intolerance (HFI) (4). Continuous exposure of these subjects to parental fructose during infancy may result in liver cirrhosis, mental retardation, and death. In most cases of HFI, final diagnosis of aldolase B deficiency is usually performed in liver biopsy specimens.

Although the advantages of using stable-isotope-labeled fructose for *in vivo* diagnosis of HFI in infants and young children is evident, such a technique has not yet been developed. A noninvasive and nonradioactive approach using  $[\text{U-}^{13}\text{C}]$ glucose was undertaken to assess the mechanism by which glucose is produced in children with glycogen storage disease type I and type III (5–8). We report here a safe tracer methodology using  $[\text{U-}^{13}\text{C}]$ fructose for studying the metabolic pathways of fructose in HFI patients and normal subjects. D- $[\text{U-}^{13}\text{C}]$ Fructose was given to normal children and HFI patients and fructose conversion to glucose was determined quantitatively by measuring  $^{13}\text{C}$  NMR resonances of plasma glucose at position C-1 coupled to C-2, as a function of the rate of  $[\text{U-}^{13}\text{C}]$ fructose infusion. Quantification of fructose metabolic steps in normal and HFI children was based on  $^{13}\text{C}$  NMR measurements of plasma glucose isotopomer populations. The isotopomer populations at position C-4 of two ( $\text{C}_3$ - $^*\text{C}_4$ - $^*\text{C}_5$ ) or three ( $^*\text{C}_3$ - $^*\text{C}_4$ - $^*\text{C}_5$ ) adjacent  $^{13}\text{C}$  atoms (or similarly at C-3) permitted us to quantitate the metabolic pathways of fructose conversion to glucose in human liver (and intestine). Our results reveal that splitting of Fru-1-P by aldolase B, the well-known pathway in the conversion of fructose to glucose, accounts for only  $\approx 50\%$  of the total amount of fructose conversion to glucose in normal subjects. Phosphorylation of Fru-1-P to  $\text{Fru}(1,6)\text{P}_2$  accounts for the other part.

## EXPERIMENTAL PROCEDURES

**Subject and Study Design.** The study included eight control infants and three HFI children. Two HFI patients were studied twice, by using different  $[\text{U-}^{13}\text{C}]$ fructose infusion rates (HFI subjects 9 and 13 and HFI subjects 11 and 12, Table 1). The control group was chosen for this study because they temporarily required supplementary nasogastric feeding due to feeding difficulties. One of the subjects was suspect for HFI but was found to be normal (control subject 4). The 9-month-old brother of HFI patient 11 (control subject 5) was found to be normal (Table 1). Two HFI patients (subjects 10 and 11) had a typical history of fructose intolerance and this diagnosis was confirmed by measurements of aldolase B

Abbreviations: HFI, hereditary fructose intolerance; Fru-1-P, fructose-1-phosphate;  $\text{Fru}(1,6)\text{P}_2$ , fructose 1,6-diphosphate; GC/MS, gas chromatography/mass spectroscopy.

<sup>¶</sup>To whom reprint requests should be addressed at: Department of Isotope Research, Weizmann Institute of Science, 76100 Rehovot, Israel.

Table 1. Doublet/singlet value of plasma glucose C-1 as a function of the [U-<sup>13</sup>C]fructose infusion rate in HFI patients and control subjects

Subject	Age, months	Glc mg/dl	Fructose infusion, mg/kg per min	d/s value of plasma Glc C-1	Glc C-1 atom % excess
Control 1	13	65	0.26	1.8 (2.0)	1.7
Control 2	17	65	0.29	1.9 (2.1)	1.6
Control 3	78	75	0.35	2.3 (2.5)	2.5
Control 4	4	90	0.38	2.4 (2.6)	2.5
Control 5	9	70	0.42	2.9 (3.2)	3.8
Control 6	17	66	0.48	3.0 (3.3)	3.4
Control 7	7	52	0.50	3.3 (3.6)	3.9
Control 8	7	80	0.27	1.8 (2.0)	2.1
HFI 9*	2	95	0.30	0.6 (0.7)	0.5
HFI 10	108	100	0.31	0.6 (0.7)	0.5
HFI 11†	17	82	0.36	0.8 (0.9)	0.9
HFI 12†	20	87	0.40	0.9 (1.0)	0.9
HFI 13*	4	95	0.50	1.3 (1.4)	1.5

Subject designations are as in Fig. 3. Doublet/singlet (d/s) values in parentheses are the calculated <sup>13</sup>C enrichment obtained by multiplying the <sup>13</sup>C natural abundance by 1.1%. Control subject 8 infused with 5-fold nonlabeled fructose: the indicated rate is of the labeled fructose only. Glc, glucose.

\*Same subject was infused at different [U-<sup>13</sup>C]fructose rates.

†Same subject was infused at different [U-<sup>13</sup>C]fructose rates.

activity in liver biopsy specimens. The patients were on a strict low-fructose diet and were in good health at the time of the study. The 2-month-old sister of HFI subject 11 (HFI subject 9) was breast-fed, and since she was not receiving cow's milk formula containing fructose or sucrose, no metabolic disorder was noticed clinically prior to the <sup>13</sup>C NMR study. The [U-<sup>13</sup>C]fructose test was repeated on this child at the age of 4 months (HFI subject 13) and both studies revealed results similar to those obtained with HFI children. After fasting (6–9 hr), each subject received a primed dose-constant nasogastric infusion of D-[U-<sup>13</sup>C]fructose (99% <sup>13</sup>C-enriched) at a rate that varied from 0.26 to 0.5 mg/kg per min. The primed dose was 25% of the total amount of D-[U-<sup>13</sup>C]fructose given throughout the study. The total amount of [U-<sup>13</sup>C]fructose given to all subjects was only 2–4% of the regular fructose load [1 g/kg (body weight)] given intravenously in fructose tolerance tests for HFI (4). One control subject (Table 1, subject 8) was given D-[U-<sup>13</sup>C]fructose (99% <sup>13</sup>C-enriched) diluted 1:5 with nonlabeled fructose. Blood samples were taken 60–90 min after the start of the infusion, when the <sup>13</sup>C enrichment of plasma glucose reached a steady state. Plasma glucose concentrations remained constant throughout the study. This study received the approval of the Human Studies Committee of Kaplan Hospital, Rehovot, and Rambam Hospital, Haifa. Informed consent was obtained from the parents of the children.

**Materials.** D-[U-<sup>13</sup>C]Fructose was obtained from D-[U-<sup>13</sup>C]glucose (99% enriched) by glucose isomerase conversion. D-[U-<sup>13</sup>C]Glucose was prepared in our laboratory from algae grown on 99%-enriched <sup>13</sup>CO<sub>2</sub> (9).

**NMR Spectroscopy.** High-resolution <sup>13</sup>C NMR spectra of deproteinized plasma samples were obtained with a Bruker AM 500-MHz spectrometer operating at 125.76 MHz with composite pulse decoupling to reduce effects from dielectric heating and to maintain the sample temperature at about 25°C. Spectra were obtained using a 5-mm <sup>13</sup>C NMR probe with the following parameters: a 60° pulse angle with a 2-s repetition time, a 26.5-kHz spectral width, and a 32 K block. Field stabilization was accomplished by locking on 6% <sup>2</sup>H<sub>2</sub>O. Signal areas were integrated with the aid of the Bruker software.

**Gas Chromatography/Mass Spectroscopy (GC/MS): Determination of Isotopic Enrichments of [U-<sup>13</sup>C]Glucose at Position C-1.** GC/MS measurements were carried out to confirm the <sup>13</sup>C enrichment data derived from the doublet to singlet ratio of <sup>13</sup>C NMR spectra of β-glucose C-1. 1,2,3,4,6-Penta-*O*-trimethylsilyl anomers of α- and β-D-glucose were derived from deproteinized plasma glucose as described (6). The GC/MS conditions for glucose, lactate, and alanine separation and their <sup>13</sup>C enrichment were as described (6, 10).

## RESULTS AND DISCUSSION

Once fructose reaches the bloodstream, it is utilized rapidly; therefore, plasma <sup>13</sup>C NMR spectra taken ≈70 min after infusion do not contain <sup>13</sup>C resonances corresponding to [U-<sup>13</sup>C]fructose. Spectra obtained with normal control subject 5 and his HFI sister (subject 12, Table 1) are shown in Fig. 1. The multiplet structure of the glucose carbon resonances are due to <sup>13</sup>C-<sup>13</sup>C coupling, either with one or two adjacent <sup>13</sup>C atoms. The <sup>13</sup>C enrichment of plasma glucose C-1 of the control subject is 3.2%, whereas that of the HFI patient is 1.0%. These values were confirmed by GC/MS (Table 1). Both subjects were subjected to similar rates of [U-<sup>13</sup>C]fructose infusion. Lactate carbons are observed as multiplet structures, indicating that their resonances are of two adjacent <sup>13</sup>C. From the triplet structure of lactate C-3 (expanded scale), the relative <sup>13</sup>C enrichment in comparison to glucose C-1 can be deduced (8). Other fructose metabolites were identified in HFI plasma, such as glycerol (its C-1 and C-3 resonances are centered at 63.5 ppm). The glycerol may be due to the activity of aldolase A on Fru(1,6)P<sub>2</sub> producing glyceraldehyde phosphate and dihydroxyacetone phosphate and to the subsequent activities of the respective dehydrog-

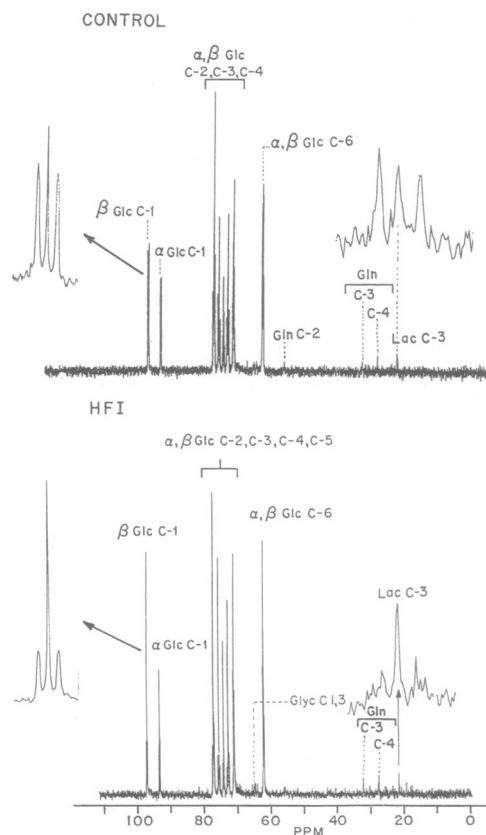


FIG. 1. Proton-decoupled <sup>13</sup>C NMR (125.76 MHz) spectra of deproteinized plasma (≈3 ml) derived from control subject 5 (in Table 1) (3600 accumulations) and from HFI patient 12 (12,000 accumulations). Glyc, glycerol.

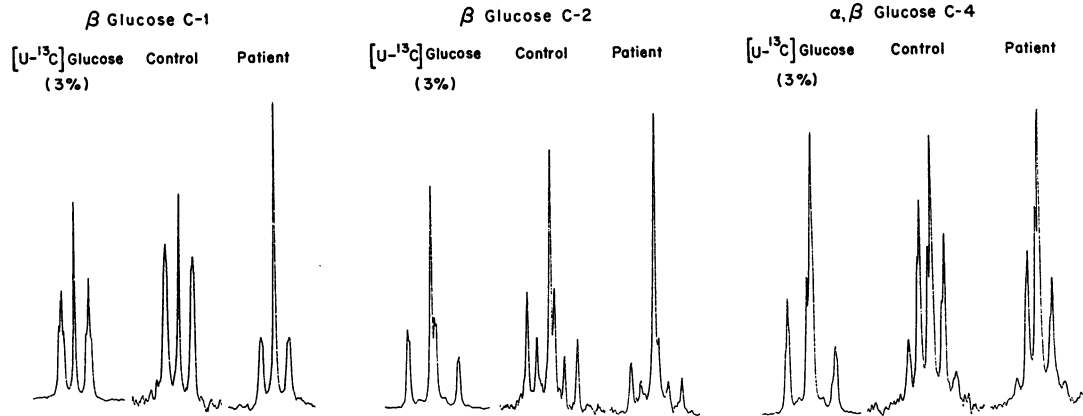


FIG. 2. <sup>13</sup>C NMR spectra of β-glucose C-1, β-glucose C-2, and α,β-glucose C-4 derived from a [U-<sup>13</sup>C]glucose/nonlabeled glucose solution from control subject 5 and from HFI subject 12 (see Table 1 and Fig. 1).

enases, resulting in *sn*-glycerol-phosphate and glycerol. <sup>13</sup>C-enrichment of glycerol is ≈0.3 atom % excess (when compared to the lactate <sup>13</sup>C splitting pattern and lactate and/or alanine GC/MS results, data not shown).

**Estimation of Fructose Conversion to Glucose in Human.** The <sup>13</sup>C-<sup>13</sup>C splitting pattern of α and β anomers of glucose C-1 reflects its <sup>13</sup>C enrichment (7, 8). In the present study, the center peak arises mainly from the nonenriched glucose carbon (1.1 atom %) and the doublet resonances of [<sup>13</sup>C]glucose arise from glucose C-1 coupled to C-2 (Fig. 2). Thus the doublet to singlet ratio of glucose C-1 is a reflection of its enrichment, as observed when GC/MS results are compared (Table 1). The <sup>13</sup>C enrichment increases as the [U-<sup>13</sup>C]fructose infusion rate is increased. Expanded views of <sup>13</sup>C NMR spectra of plasma β-glucose C-1 derived from control and HFI subjects (subjects 5 and 12, respectively, in Table 1) are compared to the [U-<sup>13</sup>C]glucose C-1 spectrum of a mixture of 3% labeled glucose (99% enriched) and 92% nonlabeled glucose ([U-<sup>13</sup>C]<sup>13</sup>C-labeled/unlabeled glucose solution) in Fig. 2. Linear regression analysis of β-glucose C-1 doublet/singlet peak areas as a function of [U-<sup>13</sup>C]fructose infusion rates is shown in Fig. 3 for eight control subjects and five measurements on three HFI subjects. A significant difference between the slopes of the curves derived from HFI patient data and from control subject measurements was observed (2.48 and 6.45, respectively), indicating that the conversion of fructose to glucose declined by 67% in HFI patients.

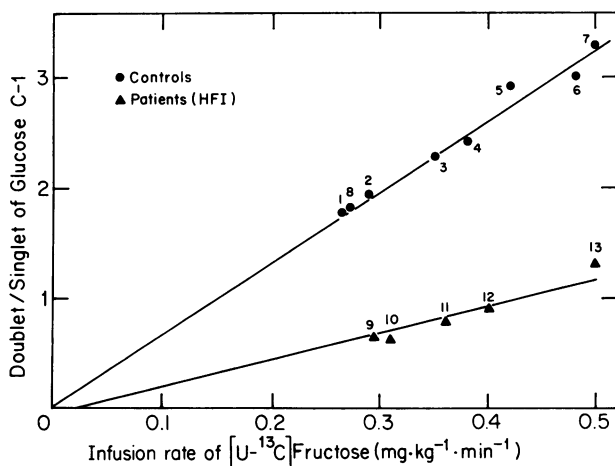


FIG. 3. Linear regression analysis of proton decoupled <sup>13</sup>C NMR of the β-glucose C-1 fraction doublet/singlet ratio as a function of [U-<sup>13</sup>C]fructose (99%) infusion rates in control subjects (●;  $R = 0.990$  and  $Y = 0.034 + 6.465X$ ) and HFI patients (▲;  $R = 0.980$  and  $Y = -0.074 \pm 2.480X$ ). Numbers refer to subjects (Table 1).

**Estimation of Fructose Metabolic Pathways: Direct and Indirect.** Glucose C-1, C-2, and C-4 splitting patterns of the [U-<sup>13</sup>C]glucose (99% enriched)/nonlabeled glucose solution were compared with the corresponding carbons of plasma [<sup>13</sup>C]glucose from control and HFI subjects (subjects 5 and 12 in Table 1) in Fig. 2. Significantly different glucose carbon splitting patterns were obtained from plasma glucose, either from control or HFI subjects, in comparison to the mixture of [U-<sup>13</sup>C]glucose and nonlabeled glucose. This is due to [U-<sup>13</sup>C]fructose conversion to glucose by the cleavage pathway to triose phosphate and interaction of three carbon compounds with tricarboxylic acid cycle intermediates, prior to their recombination to glucose. We assumed that the probability of D-[U-<sup>13</sup>C]glucose forming as a result of recombination of two molecules of [U-<sup>13</sup>C]triose phosphate was negligible, since a similar <sup>13</sup>C isotopomer pattern for glucose C-4 was observed when the infusion mixture consisted of a mixture at 20% [U-<sup>13</sup>C]fructose and 80% nonlabeled fructose (subject 8). As a consequence of a 1:5 dilution of [U-<sup>13</sup>C]triose phosphate in the intimate environment of the hepatic cell, the probability of the recombination of two molecules of triose phosphate to form [U-<sup>13</sup>C]-Fru(1,6)<sub>P</sub><sub>2</sub> should be lower by a factor of 1/5<sup>2</sup> or 0.04. Thus, in view of our findings, the contribution of two molecules of [U-<sup>13</sup>C]triose phosphate to form [U-<sup>13</sup>C]glucose can be eliminated (at least under the conditions in our study). Direct conversion of intact [U-<sup>13</sup>C]fructose through Fru-1-P to Fru(1,6)<sub>P</sub><sub>2</sub> will result in the formation of [U-<sup>13</sup>C]glucose molecules, and the <sup>13</sup>C spectra of glucose C-4 or C-3 will then exhibit a triplet resonance, similar to that of the [U-<sup>13</sup>C]glucose/nonlabeled glucose mixture, as seen in Fig. 2 and in the diagram shown in Fig. 4, isotopomer population C, for the glucose \*C<sub>3</sub>-\*C<sub>4</sub>-\*C<sub>5</sub> isotopomer. Analysis of the multiplet spectra observed for glucose C-4 (or C-3) resonances from plasma samples (Fig. 2) permits quantitation of the contributions of direct and indirect pathways for fructose conversion to glucose in human liver. For example, Fig. 4 illustrates that the five-line multiplet observed for α and β C-4 (or β C-3, data not shown) is the consequence of the presence of a mixture of isotopomers. The apparent triplet resonances are due to glucose \*C-4 coupled to \*C-3 and \*C-5, and the doublet resonances are those of glucose \*C-4 coupled to \*C-5. The singlet resonance of C-4 is mainly from the natural abundance of <sup>13</sup>C (1.1%). The relative areas of the individual components of the multiplet were measured. The ratio of the isotopomers corresponding to a triplet and doublet resonances, derived from <sup>13</sup>C NMR spectra of plasma samples obtained from eight control children, was found to be 0.89 (± 0.05), which corresponds to 46.9 (± 1.4)% direct conversion of [U-<sup>13</sup>C]fructose to [U-<sup>13</sup>C]glucose. The contribution of the

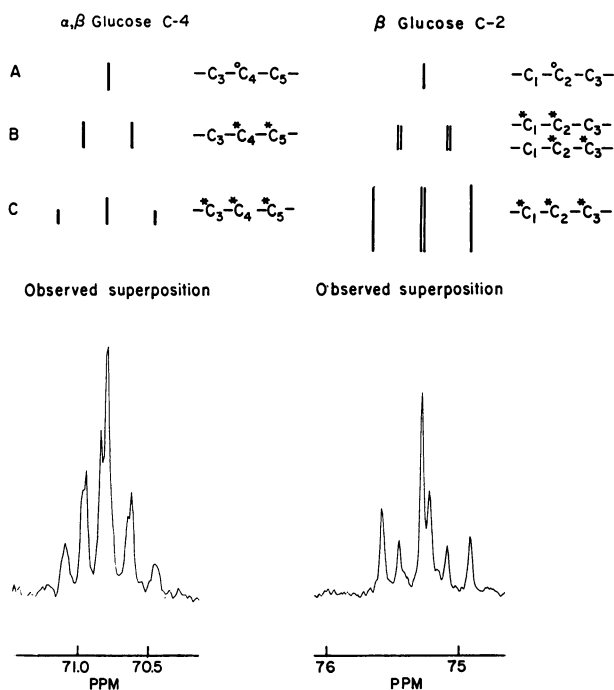


FIG. 4. Schematic presentation of isotopomer populations (A-C) of  $\alpha,\beta$ -glucose  $^*C_4$  coupled to one or two adjacent  $^{13}C$  ( $J_{34} = 39.0$  and  $41.4$  for  $\alpha$ - and  $\beta$ -glucose, respectively, and  $J_{45} = 41.2$  for  $\alpha$ - and  $\beta$ -glucose) and  $\beta$ -glucose  $^*C_2$  coupled to one or two adjacent  $^{13}C$  ( $J_{12} = 46.0$  and  $J_{23} = 40.5$  for  $\beta$ -glucose) (13). Similar  $J$  couplings were obtained from a two-dimensional  $J$ -resolved spectrum obtained from  $[U-^{13}C]$ glucose (A.G. and A.L., unpublished data). The corresponding observed superposition spectra are from a control subject, taken from Fig. 1.  $C_3-C_4-C_5$  and  $C_1-C_2-C_3$  are the natural abundance peaks of glucose C-4 and C-2, respectively. Since the center peak of the triplet resonances coincided with the natural abundance peaks, triplet resonances were calculated by multiplying the outer peak areas by 2. The splitting of the  $\alpha,\beta$ -glucose C-4 center peak is a result of partially resolved  $\alpha,\beta$ -glucose anomers. The splitting of the  $\beta$ -glucose C-2 center peak arises from the  $\beta$ -glucose C-2 natural abundance and the different  $^1J_{12}$  and  $^1J_{23}$  of the  $^*C_1-C_2-C_3$  isotopomer. The inner doublet splittings arise from  $^2J$  coupling.

singlet resonance at glucose C-4 fell slightly as a result of an increase in the rate of  $[U-^{13}C]$ fructose infusion. This is consistent with the increase in  $^{13}C$  enrichment of glucose measurement (Table 1). In HFI patients the apparent triplet/doublet ratio decreased to  $0.37 (\pm 0.02)$ ; this may be due to a decrease of the contribution of flow by the direct pathway in comparison to the indirect.

Our results indicate that the accepted mechanism for fructose conversion to glucose by splitting Fru-1-P to triose phosphate with aldolase B contributes only  $\approx 50\%$  to the total conversion of fructose to glucose in normal human subjects. In HFI patients, aldolase B activity is impaired, but aldolase A activity is not deficient (4). Since the main substrate for aldolase A activity is Fru(1,6) $P_2$ , the doublet resonances of glucose C-4 corresponding to the isotopomer population of glucose  $^{13}C_4-^{13}C_5$  (Fig. 4) may also be attributed to triose phosphate formation by the action of aldolase A on Fru(1,6) $P_2$  in HFI subjects. This hypothesis is in agreement with the suggested phosphorylation pathway of Fru-1-P to Fru(1,6) $P_2$  for both controls and HFI patients in this study. According to our data, the decrease in the total conversion of fructose to glucose that occurs in HFI patients corresponds to 33% of the total aldolase activity; this is slightly higher than the values obtained for aldolase B activity by *in vitro* enzymatic liver biopsy assay (4). Thus, our value may represent the total activity of possible residual aldolase B and aldolase A measured *in vivo* by our technique.

**Estimation of Fructose Metabolite Recycling.** This laboratory has proposed and developed approaches for measuring glucose carbon recycling using either mass spectroscopy (5, 6, 11) or  $^{13}C$  NMR spectroscopy (8). In both methods, the infused tracer was  $[U-^{13}C]$ glucose ( $>99\%$ ). An advantage of using  $[U-^{13}C]$ fructose as a tracer in gluconeogenesis studies employing  $^{13}C$  NMR is that plasma  $^{13}C$ -labeled glucose derived from the  $^{13}C$ -labeled precursor is not masked by the infused materials.

Recycling three-carbon molecules (pyruvate, lactate, and alanine) in the tricarboxylic acid cycle reflects intramolecular dilution. Thus, glucose molecules obtained from these recycled  $^{13}C$ -labeled three-carbon molecules should give different splitting patterns of glucose C-2 (or glucose C-5) than glucose molecules derived from the nonrecycled  $^{13}C$ -labeled three-carbon molecules ( $^*C_1-C_2-C_3$ ). Plasma glucose C-2 multiplet spectra, obtained from control and HFI (subjects 5 and 12, respectively, in Table 1), are compared to the spectrum of a  $[U-^{13}C]$ glucose/nonlabeled glucose mixture in Fig. 2. Quantitative analysis of peak areas of the doublet resonances obtained for glucose  $^*C_2$  coupled to  $^*C_3$  or to  $^*C_1$  and triplet resonances of glucose  $^*C_2$  coupled to  $^*C_1$  and  $^*C_3$  (as illustrated in Fig. 4) were carried out for all subjects including HFI patients. The isotopomer analysis reveals that the indirect pathway of glucose synthesis from triose phosphate (derived from  $[U-^{13}C]$ fructose) also gives three carbon molecules that are "intramolecularly" diluted, since the observed glucose spectra also demonstrates isotopomers of  $^*C_1-C_2-C_3$  and  $C_1-C_2-C_3$ . The mean value of the ratio of doublet to triplet peak areas in the glucose C-2 splitting pattern is  $3.70 (\pm 0.22)$  (derived from eight control subjects). Thus,  $21.6 (\pm 1.2)\%$  of the total fructose conversion to glucose is derived from recycled three-carbon molecules that lost only one carbon as a result of randomization by way of malate-fumarate ( $^*C_1-C_2-C_3$ ) conversion and of further randomization in the tricarboxylic acid cycle ( $C_1-C_2-C_3$ ). Although a small quantity of the infused  $[U-^{13}C]$ fructose is converted to  $[^{13}C]$ glucose in HFI subjects (33% of that in control subjects), similar isotopomer analysis of plasma glucose C-2 could be done. The ratio of doublet to triplet peak areas of HFI subjects is lower,  $2.00 (\pm 0.05)$ , which corresponds to  $33.3 (\pm 0.7)\%$  recycled three-carbon molecules of the total fructose conversion to glucose. This slightly higher value is in accordance with our finding that in the limited amount of  $[^{13}C]$ glucose produced from  $[U-^{13}C]$ fructose, the indirect pathway in this group of patients is utilized slightly more than in normal humans ( $\approx 70\%$  and  $\approx 50\%$ , respectively). A scheme illustrating glucose isotopomers derived from the  $^{13}C$  NMR splitting pattern of plasma glucose at positions C-2 and C-4, after  $[U-^{13}C]$ fructose administration, is presented in Fig. 5.

The lactate C-3 resonances (Fig. 1) reveal that lactate C-3 is coupled to C-2, consistent with the observed glucose isotopomers  $^*C_1-C_2-C_3$  and  $C_1-C_2-C_3$ . The ratio of doublet to singlet peak areas of lactate C-3 can be used to estimate  $[^{13}C]$ lactate dilution by the endogenous pool. By assuming that the singlet is derived from the naturally abundant lactate C-3 only (6), the relative  $^{13}C$  enrichment of glucose to lactate is  $\approx 3:1$ . Thus, the marked decline in  $[^{13}C]$ lactate enrichment in comparison to glucose indicates that the lactate enrichment is mostly produced from muscle glycolysis of the  $^{13}C$ -labeled glucose derived from the  $[U-^{13}C]$ fructose. The lactate C-3 resonance observed in the plasma spectra of HFI (expanded scale, Fig. 1) is only 0.2–0.3 atom % excess, as calculated from the lactate C-3 doublet/singlet peak areas. Other metabolites, alanine and glutamine, can be detected, although their concentration and  $^{13}C$  enrichment were very low.

**Suggested Metabolic Pathways for Fructose Conversion to Glucose in Humans.** Analysis of plasma glucose isotopomer

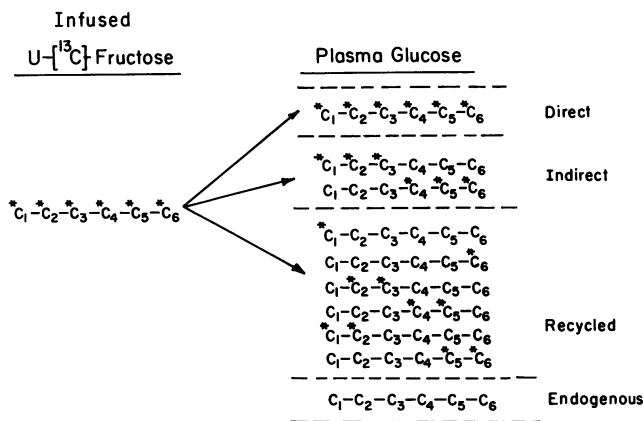


FIG. 5. Schematic presentation of labeling pattern of plasma glucose after  $[U-^{13}C]$ fructose administration into humans.

populations leads us to suggest that two main pathways are responsible for conversion of fructose to glucose in humans, a direct and an indirect phosphorylation pathway of Fru-1-P to Fru(1,6) $P_2$ ; each pathway accounts for  $\approx 50\%$  (in control subjects) of the total conversion (Fig. 6). Landau *et al.* (12) showed that in normal and HFI subjects, after intravenous administration of fructose (60 mg/kg as a bolus, containing  $[6-^{14}C]$ fructose and lactate) $[1-^{14}C]$ , similar glucose C-1/C-6 and C-3/C-4 ratios of 0.61 to 0.80 were measured in their study. These results were attributed to incomplete equilibrium of triose phosphate and to the transaldolase exchange reaction. Upon administration,  $[U-^{13}C]$ fructose is metabolized to two equivalent three-carbon units ( $^{13}C_1-^{13}C_2-^{13}C_3$  and  $^{13}C_4-^{13}C_5-^{13}C_6$ ) (dihydroxyacetone phosphate and glyceraldehyde, which is subsequently phosphorylated to glyceraldehyde phosphate). Thus, even if equilibrium of triose phosphate is incomplete, the transaldolase exchange reaction is active, or both, their effect should not be apparent (see Fig. 5). In the studies performed by Landau *et al.* (12), the glucose C-1/C-6 ratio fell by 12% and 20% in two of the HFI subjects,

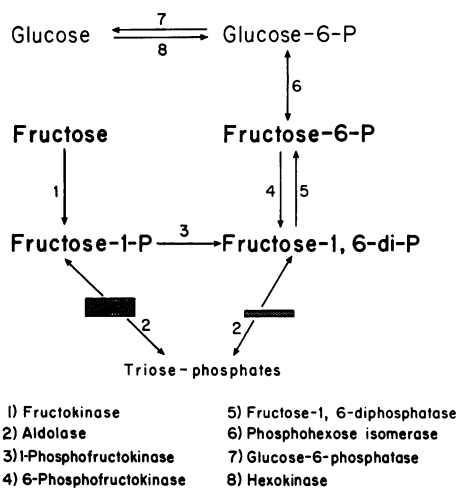


FIG. 6. Schematic presentation of fructose conversion to glucose in human liver; a suggested mechanism for direct conversion of Fru-1-P (fructose-1-P) to Fru(1,6) $P_2$  (fructose-1,6-di-P) by 1-phosphofructokinase. Glucose-6-P, glucose 6-phosphate; fructose-6-P, fructose 6-phosphate; fructose-1,6-diphosphatase, fructose-1,6-bisphosphatase.

a result that was interpreted as occurring due to fructose phosphorylation to fructose 6-phosphate. In recent studies on children with fructose-1,6-bisphosphate deficiency (A.G., A. Gutman, and A.L., unpublished data), the occurrence of an initial phosphorylation to fructose 6-phosphate does not tally with the nonlabeled glucose values observed after  $[U-^{13}C]$ fructose administration to five fructose-1,6-bisphosphatase-deficient patients. Since in these patients the deficiency is in the fructose-1,6-bisphosphatase activity but not in the hexokinase activity, phosphorylation of fructose to fructose 6-phosphate might be expected, so that  $[U-^{13}C]$ fructose administration to fructose-1,6-bisphosphatase-deficient subjects would indeed result in  $^{13}C$ -enriched glucose. However, our findings show that, in fructose-1,6-bisphosphatase-deficient children, only the gluconeogenic precursors, lactate, alanine, and glycerol are  $^{13}C$ -enriched but not the glucose itself.

The apparent anomaly of a decrease in the direct conversion of Fru-1-P to Fru(1,6) $P_2$  in the HFI group and its association with an overall lower rate of metabolism of fructose and a lower rate of conversion of fructose to glucose are not clear.

In summary, an approach to a quantitative determination of the steps in the fructose to glucose conversion pathway in normal and HFI children, by analysis of  $[^{13}C]$ glucose isotopomers in plasma after  $[U-^{13}C]$ fructose administration, is presented. A direct pathway from fructose, bypassing Fru-1-P aldolase to Fru(1,6) $P_2$  by 1-phosphofructokinase, which accounts for 47% and 27% of the conversion in control and HFI children, respectively, is suggested. The accepted pathway of fructose conversion to glucose, by Fru-1-P aldolase to triose phosphate, accounts for only 53% and 75% of the conversion in normal and HFI subjects, respectively. The significantly lower (by 67%) conversion of fructose to glucose in HFI as compared to control subjects after  $[U-^{13}C]$ fructose ( $\approx 20$  mg/kg) administration can serve as the basis of a safe diagnostic test for patients suspected of inborn errors of fructose metabolism.

This work is dedicated to the memory of Prof. Edgar Lederer (1908–1988). We thank Ms. M. Dorsman for synthesis of D- $[U-^{13}C]$ fructose. This work was partly supported by grants from the Israeli Ministry of Health and the Israel Academy of Science to A.L.

- Van den Berghe, G. (1986) *Prog. Biochem. Pharmacol.* **21**, 1–32.
- Hers, H. G. (1957) *Le metabolisme du fructose* (Edition Arscia, Brussels).
- Hers, H. G. (1955) *J. Biol. Chem.* **214**, 373–381.
- Gitzelmann, R., Steinmann, B. & Van den Berghe, G. (1985) *The Metabolic Basis of Inherited Disease* (McGraw Hill, New York), 5th Ed., pp. 118–139.
- Kalderon, B., Lapidot, A., Korman, S. H. & Gutman, A. (1988) *Biomed. Environ. Mass Spectrom.* **16**, 305–308.
- Kalderon, B., Korman, S. H., Gutman, A. & Lapidot, A. (1989) *Am. J. Physiol.* **257**, E346–E353.
- Lapidot, A., Kalderon, B., Korman, S. H. & Gutman, A. (1988) *Soc. Magn. Reson. Med.* **1**, 249.
- Kalderon, B., Korman, S. H., Gutman, A. & Lapidot, A. (1989) *Proc. Natl. Acad. Sci. USA* **86**, 4690–4694.
- Lapidot, A. & Kahana, Z. (1986) *Trends Biotech.* **4**, 2–4.
- Lapidot, A. & Nissim, I. (1980) *Metabolism* **29**, 230–239.
- Kalderon, B., Gopher, A. & Lapidot, A. (1986) *FEBS Lett.* **204**, 29–32.
- Landau, B. R., Marshall, J. S., Craig, J. W., Hostetler, K. Y. & Genuth, S. M. (1971) *J. Lab. Clin. Med.* **78**, 608–618.
- Breitmaier, E. & Voelter, W. (1987) *Carbon-13 NMR Spectroscopy* (VCH, New York), 3rd Ed., p. 148.